

EXPERIMENTAL MODELING OF THE FLASHOVER OF POLLUTED INSULATOR WITH THE PRESENCE OF A METAL PLATE USING RSM TECHNIQUE

Mohamed BOUHMAMA¹ Samir FLAZI² Farid MILOUA¹
Yassine BELLEBNA¹ Amar TILMATINE¹

¹APELEC Laboratory, DjillaliLiabes University of Sidi Bel-Abbes.22000, Algeria;

²LGEO Laboratory, University of science and technology, Oran.31000, Algeria;

Email : atilmatine@gmail.com , yassinebellebna@yahoo.fr

Abstract — *The flashover of polluted insulators has been the subject of many experimental and numerical research papers. Several mathematical models of the flashover voltage have been proposed according to the current, the discharge length, the electrolyte length and the resistivity. However, there is no model based on the geometric factors of the electrolyte channel and their interaction, such as the width and the depth. Furthermore, as a very few research papers about the discharge elongation in the presence of a metal object between the electrodes have been published, the aim of the present work is the modeling of the flashover voltage in the presence of a metal plate, dipped in the electrolyte or placed on its surface. Two mathematical models were obtained using response surface modeling technique, which were used for the analysis of the geometric factors effect on the flashover discharge.*

Keywords: Power systems, Polluted insulator, Flashover, Response surface modelling, Experimental Designs.

1. Introduction

The flashover of a high voltage polluted insulator causes lines short-circuit to ground, due to the propagation of an electrical discharge on its surface. A conducting electrolyte is created on the insulator surface due to the combination of the dry pollution deposited on the surface with the ambient humidity, causing therefore the flow of a leakage current [1-3]. The non-uniform distribution of the leakage current at the polluted surface of the insulator results in non-uniform heating of the pollution layer causing the formation of dry bands, accompanied by the ignition of partial discharges which transform

to complete flashover [4-5].

Due to the development of high energy power grids, flashover of insulators polluted with various industrial contaminants is considered nowadays as an important problem for the safe operation of transmission lines and the design of the external insulation.

Mathematical models to predict the critical flashover voltage exist and are primarily directed towards the comprehension of the development of electric arcs on the insulator surface. Such modeling can be useful for designing high-performance insulators, thus minimizing time consuming experimental laboratory work. However, the development of a mathematical model still remains quite difficult due to the complex phenomena of the flashover [6-9].

A few research papers about the discharge elongation, in the presence of a conductive object between the electrodes, dipped in the electrolyte or placed on its surface, have been published. The results of such studies have shown that the introduction of the object affects the conditions of the discharge propagation [10-12]. However, the analysis of the influence of each factor is not sufficient for a full understanding of the phenomenon, since it does not take into account the effect generated by the interaction between the various factors. On the other hand, several mathematical models of the flashover voltage have been proposed according to the current, the discharge length, the electrolyte length and the resistivity. However, there is no model based on the geometric factors of the electrolyte channel, such as the width and the depth. Furthermore, no model has been proposed in the presence of a metallic plate

placed in the path of the flashover discharge.

The objective of this paper is to carry out an experimental modeling of the flashover voltage measured on an Obenaus-model laboratory-cell, using the experimental designs methodology. Furthermore, we analyzed the influence of the presence of a metallic plate by performing two centered-face composite designs of the two configurations, with and without the presence of the plate.

2. Material and methods

2.1 Experimental setup

The experimental setup, shown in Fig.1, delivers a variable DC high voltage up to 30 kV with a maximum current of 2 A. The voltage supplied by means of a HV capacitor bank of total capacitance $C = 16.7\mu\text{F}$, is charged to the desired value by a variable step-up 220V/30 kV transformer, through a diode rectifier bridge. The transformer is supplied by using a 0-220 V variac in order to control the high voltage output. A measuring set, consisting of a storage oscilloscope (Leader, LBO-5825) and a HV probe (Tektronix, P6015A), serve to measure the applied voltage.

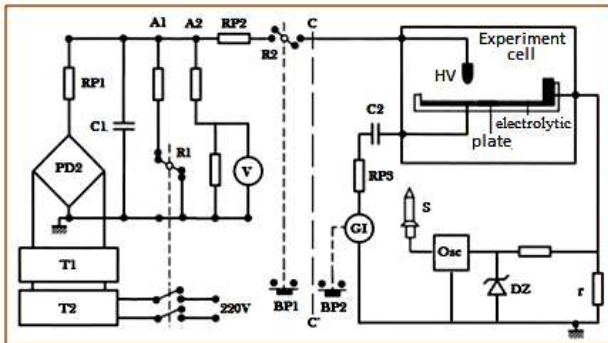


Fig 1: Descriptive schematic of the experimental setup

- T1** – HV transformer (220 V/ 30 kV)
- T2** – Variac (autotransformer) 0/220 V
- PD2** – Single-phase HV bridge rectifier
- C1** – Battery of 10 capacitors $5C = 1.67\mu\text{F} - 30 \text{ kV}$
- A1** – Automatic discharge circuit of the capacitor C1
- A2** – Scaling resistor.
- R1, R2** – High voltage relay.
- GI** – Pulse generator.
- BP1** – Control push-button of the pulse generator;
- BP2** – Control push-button of the HV discharge (R2).
- C2** – Capacitor of insulation ($\approx 1000\text{pF}$).
- Osc** – LEADER oscilloscope memory
- S** – Measuring HV probe; Tektronix P6015
- RP1, RP2 and RP3** – Resistors of protection
- R** – Resistor (0.7Ω) for the current measurement

The experiments were performed using a laboratory “Obenaus-model” cell representing the non-conducting surface of the insulator. A rectangular channel of constant length $L=8 \text{ cm}$, but variable width a and depth p , is made on a Plexiglas plate of thickness 2 cm (Fig.2). The channel is filled with an electrolyte, which is a mixture of distilled water and sodium chloride salts ($\text{NaCl} + \text{H}_2\text{O}$), whose dosage enables to vary the resistivity of the electrolyte. The HV electrode is placed above the electrolytic surface at a fixed height $h=0.3 \text{ cm}$, and is distant 8 cm from the ground electrode (Fig.2). In addition, a metal plate of width a and constant length $l=1 \text{ cm}$, but with variable thickness e , is placed on the discharge path between the two electrodes.

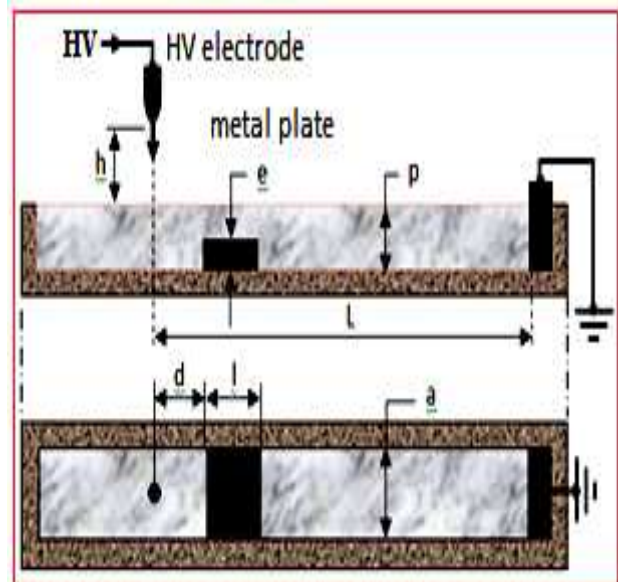


Fig 2: Descriptive representation of the experimental cell and its dimensions

(Top) Front view; (Bottom) Top view

Variable sizes: width a and depth p of the cell, thickness e of the plate

Constant sizes: height of the HV electrode $h=0.3 \text{ cm}$;
Length of the electrolyte $L=8 \text{ cm}$; Length of the metal plate $l=1 \text{ cm}$

The experiments were performed using several experimental cells of different geometric dimensions, having the same constant length $L=8 \text{ cm}$, but different values of width a , depth p and plate thickness e . After each performed test, a new electrolytic solution is replaced and the capacitors are charged again to a voltage $V = V_d$. The critical flashover voltage V_c measured corresponds to the smallest value of the voltage V_d causing the flashover.

The work done in this paper was related to the analysis of three factors which are the channel width a (cm), the channel depth p (cm) and the per unit length resistance r (kΩ/cm). Resistance r was considered with the geometric factors because its value changes with the cell dimensions. Three “one-factor-at-a-time experiments”, followed by two composite designs (without and with lame), were performed following the following experimental procedure:

- 1) Fixing the variation domain of the factors; 2) modeling step: searching the optimal point corresponding to the lowest value of V_c ; and 3) analyzing the influence of the factors.

2.2 Experimental Designs Methodology

The methodology of the experimental designs is particularly used to determine the number of experiments to be carried out according to a well-defined objective, to study several factors simultaneously and to evaluate the respective influence of the factors and their interactions [13-16].

The most suitable design, which models the process with high precision, should be set before starting the experiments. In the present work, the Composite Centred Faces design (CCF), which gives quadratic models, was adopted. A quadratic dependence is determined between the output function to optimize (response) and the input variables u_i ($i = 1, \dots, k$) (factors):

$$y = f(u_i) = c_0 + \sum c_i u_i + \sum c_{ij} u_i u_j + \sum c_{ii} u_i^2 \quad (1)$$

Knowing that Δu_i and u_{i0} are respectively the step of variation and the central value of factor i , reduced centred values of input factors may be defined by the following relation:

$$x_i = (u_i - u_{i0}) / \Delta u_i \quad (2)$$

With these new variables, the output function becomes:

$$y = f(x_i) = a_0 + \sum a_i x_i + \sum a_{ij} x_i x_j + \sum a_{ii} x_i^2 \quad (3)$$

The coefficients can be calculated or estimated by a data-processing program, in such a way to have a minimum variance between the predictive mathematical model and the experimental results.

MODDE 5.0 software (U metrics AB, Umea, Sweden) was used, which is a Windows program for the creation and the evaluation of experimental designs [17]. The program calculates the

coefficients of the mathematical model and identifies the best adjustments of the factors for optimizing the response. Moreover, the program calculates two significant statistical criteria which make it possible to validate or not the mathematical model, symbolized by R^2 and Q^2 . For a model to be validated, both parameters should be high close to the unit, and preferably not separated by more than 0.2–0.3.

2.3 Design of flashover Experiments

The methodology of experimental designs is a powerful tool for screening and optimization. Screening experiments are designed in this paper to identify the domain of variation of the three factors (classical “one-factor-at-a-time” experiments). The optimization stage of the procedure should enable the determination of factor values for which the flashover voltage is a minimum

1) Variation domain of the factors

The variation limits of the three factors are defined by following experiments called “one-factor-at-a-time-experiments” obtained by varying one factor and keeping the two other constant at fixed values, in both cases without and with the metallic plate. The obtained results are represented in Table 1.

Obtained results in this section served to the definition of the following variation domain of the three factors for modeling step:

Width a : $a_{\min} = 2$ cm; $a_{\max} = 4$ cm

Depth p : $p_{\min} = 0.3$ cm; $p_{\max} = 0.6$ cm

Resistance r : $r_{\min} = 2.5$ kΩ/cm; $r_{\max} = 5$ kΩ/cm

Table 1: Obtained values of V_c according to width a , depth p and resistance r

		V_c (kV)	
		Without plate	With plate
a (cm) ($d= 0.45$ cm) ($r= 3.75$ kΩ/cm)	1	9	15
	2	10	17.5
	3	11	18
	4	11.5	17
p (cm) ($r= 3.75$ kΩ/cm) ($a= 2$ cm)	0.3	9.5	17
	0.45	10	17.5
	0.6	11	18
r (kΩ/cm) ($p= 0.45$ cm) ($a= 2$ cm)	2.5	9.5	17
	3.75	10	16.5
	5.0	11	16

2) Modeling of the flashover voltage

The identification of the optimal point (a_o, p_o and r_o) by using a CCF design was performed; the two levels “max” and “min” are the limits established in previous section for each of the three variables (a_{min}, a_{max}), (p_{min}, p_{max}) and (r_{min}, r_{max}), the central point (a_c, p_c and r_c) being calculated as follows:

$$a_c = (a_{min} + a_{max}) / 2 = (2 + 4) / 2 = 3 \text{ cm} \quad (4)$$

$$p_c = (p_{min} + p_{max}) / 2 = (0.3 + 0.6) / 2 = 0.45 \text{ cm} \quad (5)$$

$$r_c = (r_{min} + r_{max}) / 2 = (2.5 + 5.0) / 2 = 3.75 \text{ k}\Omega / \text{cm} \quad (6)$$

After the identification of the variation domains of the factors, two experimental designs were performed for both cases, without and with the metallic plate. The obtained results of the voltage V_{c0} (without plate) and V_{c1} (with plate) are given in tables 2 and 3 respectively. In the configuration without the metal plate (Table 3), a fourth factor was considered which is the thickness e of the plate ($e=0.15, 0.3$ and 0.225 cm). In this case of four factors, the experimental design comprises 27 experiments.

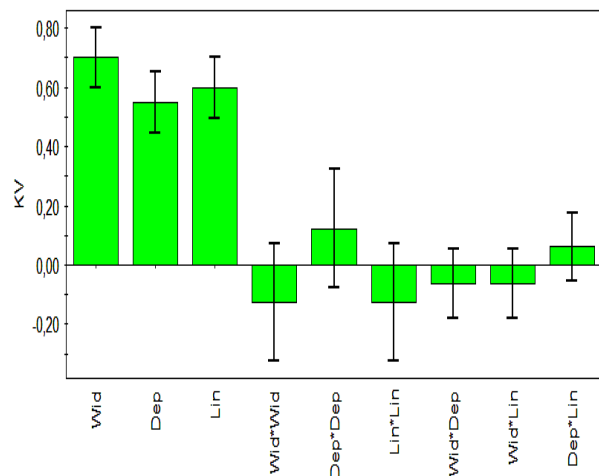
Table 2: Obtained results of the CCF design without the metal plate

Exp. N°	a (cm)	P (cm)	r (k Ω /cm)	V_{c0} (kV)
1	2	0.3	2.5	9.0
2	4	0.3	2.5	10.5
3	2	0.6	2.5	10.0
4	4	0.6	2.5	11.5
5	2	0.3	5.0	10.0
6	4	0.3	5.0	11.5
7	2	0.6	5.0	11.5
8	4	0.6	5.0	12.5
9	2	0.45	3.75	10.0
10	4	0.45	3.75	11.5
11	3	0.3	3.75	10.5
12	3	0.6	3.75	11.5
13	3	0.45	2.5	10.0
14	3	0.45	5.0	11.5
15	3	0.45	3.75	11.0
16	3	0.45	3.75	11.0
17	3	0.45	3.75	10.8

Table 3: Obtained results of the CCF design with the metal plate

Exp No	a (cm)	P (cm)	r (k Ω /cm)	e (cm)
1	2	0.3	2.5	0.15
2	4	0.3	2.5	0.15
3	2	0.6	2.5	0.15
4	4	0.6	2.5	0.15
5	2	0.3	2.5	0.3
6	4	0.3	2.5	0.3
7	2	0.6	2.5	0.3
8	4	0.6	2.5	0.3
9	2	0.3	5	0.15
10	4	0.3	5	0.15
11	2	0.6	5	0.15
12	4	0.6	5	0.15
13	2	0.3	5	0.3
14	4	0.3	5	0.3
15	2	0.6	5	0.3
16	4	0.6	5	0.3
17	2	0.45	3.75	0.225
18	4	0.45	3.75	0.225
19	3	0.3	3.75	0.225
20	3	0.6	3.75	0.225
21	3	0.45	3.75	0.15
22	3	0.45	3.75	0.3
23	3	0.45	2.5	0.225
24	3	0.45	5	0.225
25	3	0.45	3.75	0.225
26	3	0.45	3.75	0.225
27	3	0.45	3.75	0.225

The coefficients of the obtained mathematical models proposed by software MODDE.05, represented by the plotted diagrams in Fig.3, show that the coefficients of voltage V_{c1} (with lame) are much greater than voltage V_{c0} .



a) Without lame

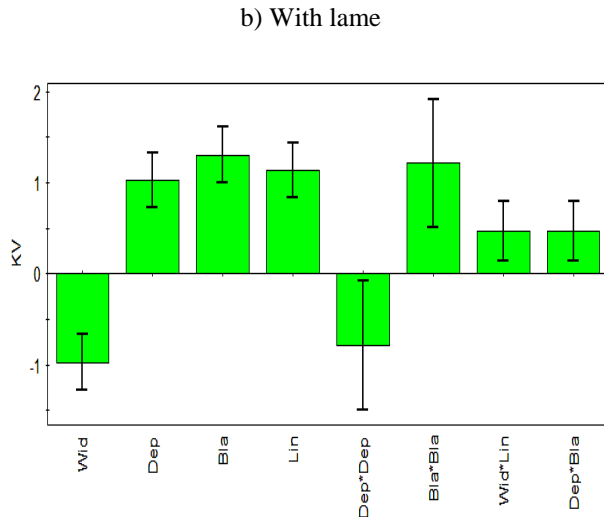


Fig.3: Diagram of the plotted coefficients of the mathematical models

There are currently two different hypotheses about the propagation of the flashover discharge. According to the majority of authors, the vertical starting discharge, which initiates between the high voltage electrode and the electrolytic surface has a cylindrical shape. According to this hypothesis, the discharge propagates on the polluted surface until flashover while keeping such cylindrical shape. It progresses due to the ionisation of the air that only occurs in the area of the discharge foot [5], [11].

However, according to Flazi's hypothesis, after initiation of the vertical cylindrical discharge, the propagation is caused in this case by the ionization of air which happens not only near the foot region of the discharge but around all the body of the discharge (Fig.4). This is caused by the electric field lines, which become current lines after ionization [7-9].

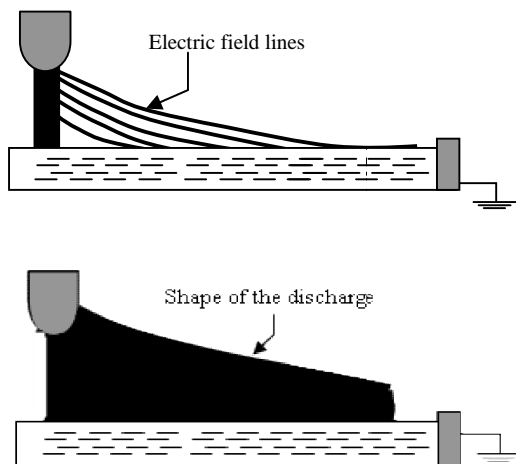
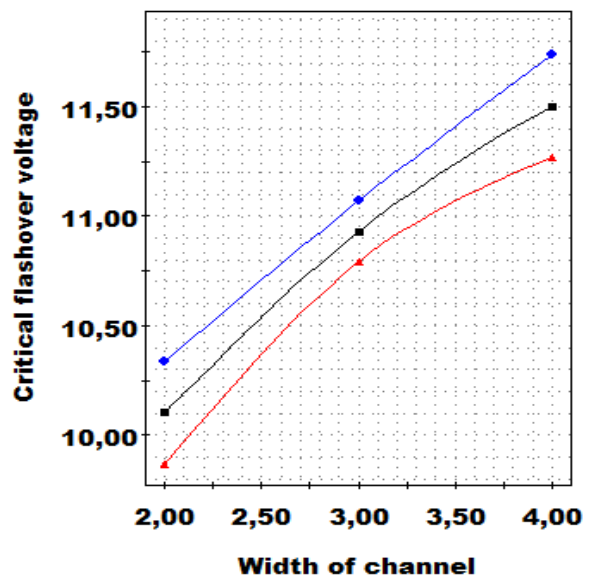


Fig 4: Evolution of the discharge according to Flazi's hypothesis

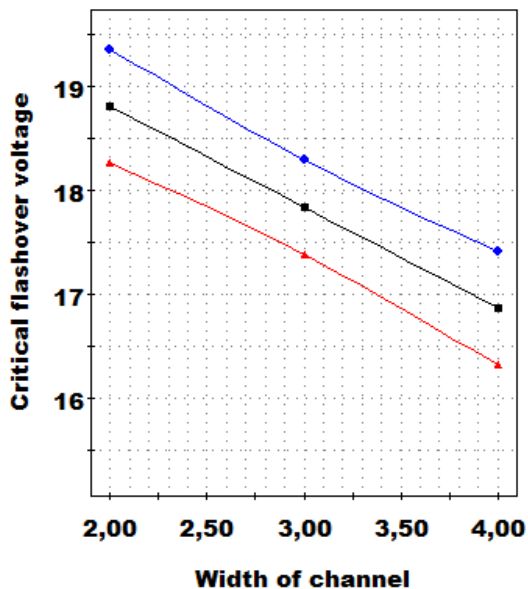
The distribution of the electric field lines around the vertical starting discharge. According to Flazi's hypothesis, the electric field lines extend to the space between the discharge column and the electrolyte, touch the electrolyte surface and become in "short circuit" state remaining constant along the plate. Indeed, during the flashover, the potential measured at the surface of the electrolyte is gradually increased during the propagation of the discharge [18-19]. In the presence of the metal plate, which represents an equipotential surface, the potential on the plate remains constant, which results in the increasing of the flashover voltage.

Furthermore, no interaction between the three factors was observed for V_{c0} . At the opposite, in the presence of the metal plate, there is a strong interaction between all the factors. This is due to the fact that the presence of the plate provides a physical link between the geometric dimensions of the channel. Without the metal plate

Prediction diagrams plotted with the software (Fig.5), show that the variation of the flashover voltage according to the channel width is clearly different with and without the presence of the metal plate. With the plate, the voltage V_{c1} decreases significantly with the width of the electrolyte due to the constriction effect of the current lines. The tightening of the current lines at the surface of the electrolyte layer, resulting for small values of a , is more important in the presence of the metal plate, causing thus the increasing of the critical voltage.



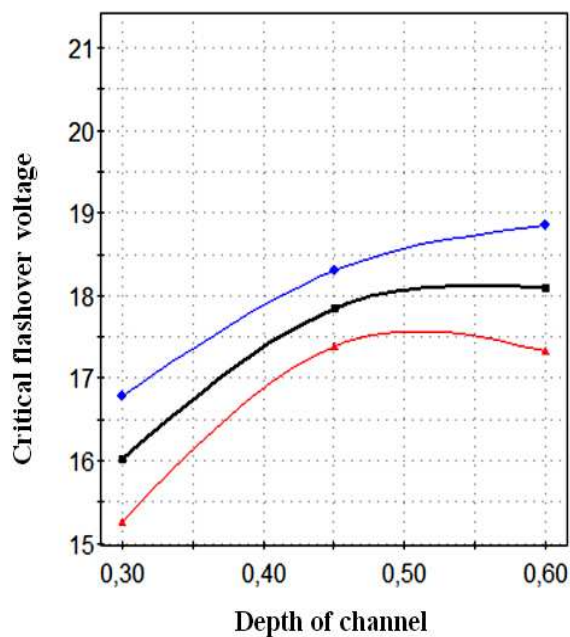
a) Without metal plate



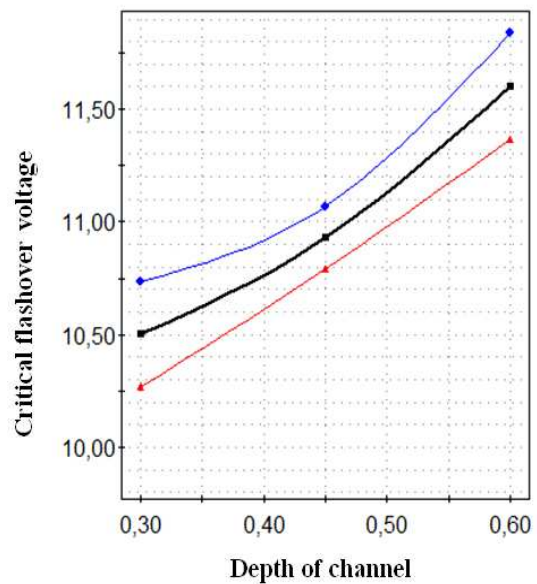
b) With metal plate

Fig.5: Predictive plots of the voltage according to the channel width

a) Without the metal plate b) with the metal plate



a) Without metal plate

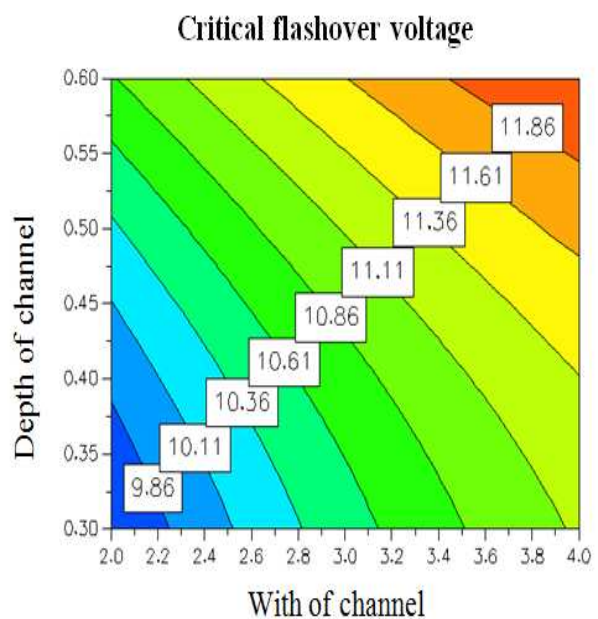


b) With metal plate

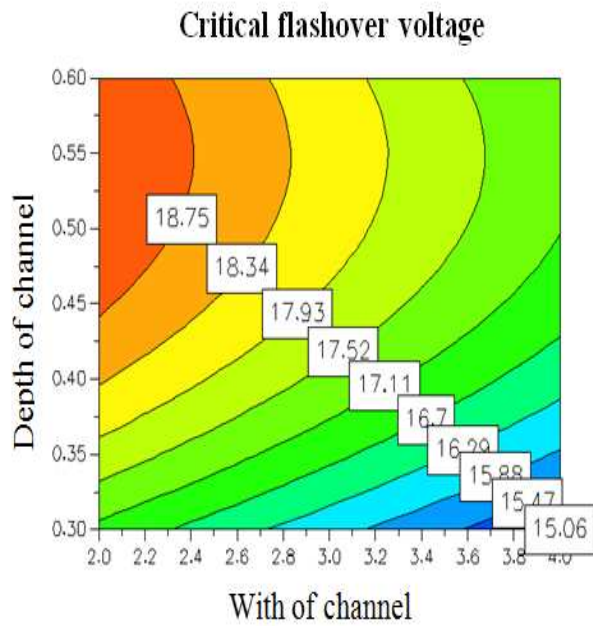
Fig.6: Predictive plots of the voltage according to the channel depth

a) Without the metal plate b) with the metal plate

As seen in Figure.6, the variation of voltage U according to the channel depth is more likely quadratic in the presence of the lame while it's almost linear without it. In the former case, the voltage is too high that the electric field lines beyond $V=18$ kV reach the ground electrode, causing therefore the flashover.



a)



b)

Fig.7: Iso-response contours plotted with MODDE.05
a) without the metal plate b) with the metal plate

Iso-response contours plotted with MODDE.05 make it possible to analyze and deduce the value ranges of the factors for which the maximum flashover voltage is obtained. The iso-response contours plotted in Fig.7, representing the influence of width a and depth p on the flashover voltage, point out that in the presence of the plate, the effect of the channel depth is greater compared with the case without plate. According to Fig.5, the flashover without plate occurs at high values of the voltage for width $a = (3.5 \dots 4 \text{ cm})$ and depth $p = (0.55 \dots 0.6 \text{ cm})$. In the presence of the metal plate, it's quite different: the flashover voltage V_{cl} becomes higher for small values of the width ($2 \dots 2.4 \text{ cm}$) and high values of channel depth ($0.44 \dots 0.6 \text{ cm}$).

When comparing the effect of the channel depth and the blade thickness (Fig.8), we notice that beyond $e = 0.22 \text{ cm}$ the effect of the blade thickness is considerably more significant than a which becomes negligible.

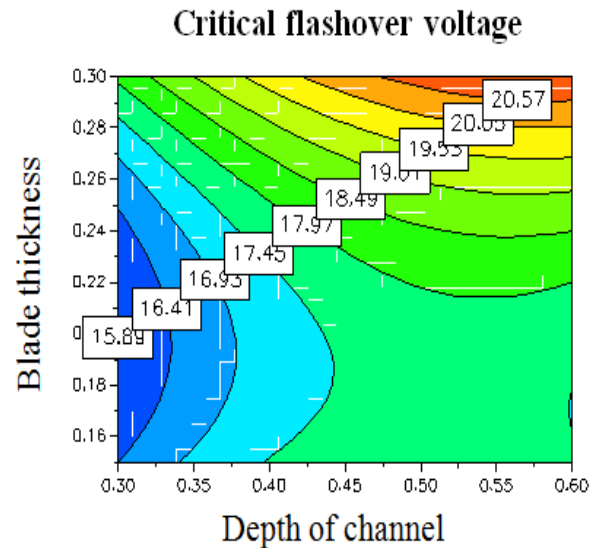


Fig.8. Effect of depth and with channel on the voltage of flashover

3) Experimental validation

The software offers the possibility to identify the optimal values of the factors which should give the highest flashover voltage. It contains an optimization routine which proposes the optimal values of factors by maximizing V_c . According to this model, the optimum of the process (i.e., maximizing the voltage V_c) should be obtained for $a = 2 \text{ cm}$, $d = 0.6 \text{ mm}$, $e = 3 \text{ mm}$ and $r = 5 \text{ k}\Omega/\text{cm}$ corresponding to $V = 22.7 \text{ kV}$ (Figure 9). "iter" is the number of iterations and "log (D)" is the Log of overall distance to the target; the value of Log (D) equals zero when all responses are between Target and Limit. The smaller Log (D), the better is the result. Log (D) becomes negative when the values of all responses are still closer to the Target (Modde 5.0 1999).

Iteration: 5003 Iteration slider: <input type="text"/>							
	1	2	3	4	5	6	7
	Width of channel	Depth of channel	Blade thickness	Lineic resistance	Critical flashover voltage	iter	log(D)
1	2,0002	0,5032	0,15	5	19,4939	5003	1,2314
2	2,0203	0,5722	0,2998	4,9887	22,6776	5000	-0,5254
3	2	0,504	0,15	5	19,4939	5001	1,2314
4	2	0,5997	0,2989	4,9801	22,6443	2020	-0,4678
5	2,0079	0,5821	0,2998	4,9962	22,7004	5000	-0,5673
6	2	0,587	0,297	4,9985	22,5537	5001	-0,3281
7	2	0,6	0,3	5	22,7185	1062	-0,602
8	2,0003	0,5744	0,2992	4,9912	22,658	3143	-0,4911

Fig. 9. Results of the optimization routine of MODDE 5.0 for maximization of the flashover voltage.

Conclusion

The flashover discharge propagating to the surface of an electrolyte was analyzed in the presence of a metal strip placed between the high voltage and the ground electrodes. Using the RSM modeling method, a mathematical model based on the geometric sizes was obtained and used for analysis and prediction. On the other hand, the flashover voltage in the presence of the plate is much higher, because the distribution of the field lines around the discharge is modified due to the fact that the potential of the metal plate surface remains invariable.

References

1. Sundararajan, R., & Gorur, R. S. (1993). Dynamic arc modeling of pollution flashover of insulators under dc voltage. *IEEE Transactions on electrical insulation*, 28(2), 209-218.
2. He, L., & Gorur, R. S. (2016). Source strength impact analysis on insulator flashover under contaminated conditions. *IEEE Transactions on Dielectrics and Electrical Insulation*, 23(2), 1005-1011.
3. Slama, M. E. A., & Beroual, A. (2015). Behavior of AC High voltage polyamide insulators: Evolution of leakage current in different surface conditions. *Advances in Electrical and Electronic Engineering*, 13(2), 74.
4. Saadati, H., Werle, P., Gockenbach, E., Borsi, H., & Seifert, J. M. (2016, June). Flashover performance of polluted composite insulators under AC and hybrid AC/DC field stress. In *IEEE Electrical Insulation Conference (EIC), 2016* (pp. 170-173). IEEE.
5. Nekahi, A., McMeekin, S. G., & Farzaneh, M. (2016, June). Influence of dry band width and location on flashover characteristics of silicone rubber insulators. In *IEEE Electrical Insulation Conference (EIC), 2016* (pp. 73-76). IEEE.
6. Sundararajan, R., & Gorur, R. S. (1993). Dynamic arc modeling of pollution flashover of insulators under dc voltage. *Electrical Insulation, IEEE Transactions on*, 28(2), 209-218.
7. Ghosh, P. S., & Chatterjee, N. (1995). Polluted insulator flashover model for ac voltage. *Dielectrics and Electrical Insulation, IEEE Transactions on*, 2(1), 128-136.
8. Aydogmus, Z., & Cebeci, M. (2004). A new flashover dynamic model of polluted HV insulators. *Dielectrics and Electrical Insulation, IEEE Transactions on*, 11(4), 577-584.
9. Dhahbi-Megriche, N., Beroual, A., & Krähenbühl, L. (1997). A new proposal model for flashover of polluted insulators. *Journal of Physics D: Applied Physics*, 30(5), 889.
10. Swift, D. A. (1980). Flashover across the surface of an electrolyte: arresting arc propagation with narrow metal strips. *Physical Science, Measurement and Instrumentation, Management and Education-Reviews, IEE Proceedings A*, 127(8), 553-564.
11. R. Wilkins and A.A.J. Al-Baghdadi, "Arc Propagation along an Electrolytic Surface", *Proc. IEE*, Vol. 118, pp. 1886-1892, 1971.
12. S. Flazi, N. Boukhennoufa and A. Ouis, "Critical Condition of DC Flashover on a Circular Sector Model", *IEEE Transactions on Dielectrics and Electrical Insulation* Vol. 13, No. 6, pp. 1335-1341, December 2006.
13. N.L. Frigon, and D. Mathews, "Practical Guide to Experimental Design", New York: Wiley, 1996.
14. G. Taguchi, "System of Experimental Designs", New York: Kraus International Publications, 1987.
15. L. Eriksson, E. Johansson, N. Kettaneh-Wold, C. Wikström, and S. Wold, "Design of Experiments. Principles and Applications". Learnways AB, Stockholm, 2000.
16. L. Eriksson, E. Johansson, N. Kettaneh, C. Wikström et S. Wold, "Design of experiments". *Umetrics Academy, Sweden*. 2000.
17. MODDE.05, "User guide and tutorial". *Umetrics*, 1999.
18. S. Flazi, "Etude du contournement électrique des isolateurs HT pollués. Critères d'élongation de la décharge et dynamique du phénomène", Thèse de doctorat es Sciences Physiques, Université Paul Sabatier, Toulouse, France.
19. Flazi, S.; Boukhennoufa, N.; Hadi, H.; Taleb, F.; The criterion of DC flashover on a circular sector models. Conference on [Electrical Insulation and Dielectric Phenomena, 2003. Annual Report.](#) 2003 Page(s):277 – 280.